

TIME RESOLVED FIELD EMISSION DETECTION DURING ESS CRYOMODULE TESTS

Enrico Cenni[†], Matthieu Baudrier, Guillaume Devanz, Luc Maurice, Olivier Piquet
CEA Université Paris-Saclay, Gif-sur-Yvette, France

Abstract

At CEA-Saclay we are currently testing the European Spallation Source (ESS) high beta cryomodules (CM). Each cryomodule is equipped with four superconducting elliptical cavities with their ancillaries (fundamental power couplers (FPC), frequency tuners and magnetic shields). The cavity is designed to accelerate protons with relativistic speed about $\beta=0.86$ and operate at an accelerating field of 19.9MV/m. During cryomodule test, operational parameters are inspected by powering up one cavity at the time. A dedicated gamma ray detection system has been designed and installed around the cryomodule in order to have a more precise insight into field emission phenomenon occurring during cryomodule operation. Recently we were able to obtain time resolved data concerning radiation emerging from the cavities due to field emission.

INTRODUCTION

In addition to the production of the 30 medium and high beta cryomodules of the European Spallation Source (ESS) LINAC, CEA performs the high RF power tests of two prototype CMs and of the three first CMs of each type assembled in Saclay. CEA currently tested two CM prototypes [1] and three from the medium beta section series, which will be re-tested at ESS test stand. Part of the testing operation consists in assessing the dose rate around the CM during operation [2]. At CEA we keep developing detectors, simulation codes and analysis tools in order to better understand field emission phenomena during CM testing and detect possible source of contamination on the cavity surface.

We present here the most recent application of plastic scintillator for gamma detection during the first two high beta series cryomodule tests (*i.e.* CM31 and CM32). The four cavities installed in the cryomodule were manufactured and prepared by Research Instrument under the supervision of UKRI Daresbury. The string assembly was carried out at CEA Saclay by a subcontractor, while the power test was performed by CEA staff [3].

EXPERIMENTAL SET UP

In Saclay we are equipped with a 704 MHz cryomodule test stand where it is possible to assess their performance by operating close to working conditions. A first set up has been described in previous publications [4,5], here we will focus on the newly designed gamma detection system developed at CEA.

Cavities and Cryomodule

The cryomodule accommodates four high beta cavity manufactured with fine grain high purity niobium [6]. In Table 1 are summarized the most significant cavity RF parameters.

Table 1: Design Parameters for High Beta Cavities [6]

Design parameters	Value
Geometrical beta - β_{geom}	0.86
Nominal gradient E_{acc} [MV/m]	19.9
Q_0 at nominal gradient	$>5 \times 10^9$
G [Ω]	241
R/Q [Ω]	435
$E_{\text{pk}}/E_{\text{acc}}$	2.2
$B_{\text{pk}}/E_{\text{acc}}$ [mT/(MV/m)]	4.3
$E_{\text{pk}} @ \text{nominal } E_{\text{acc}}$ [MV/m]	43.8
$B_{\text{pk}} @ \text{nominal } E_{\text{acc}}$ [mT]	85.6

Gamma and Neutron Diagnostic Systems

Part of the testing activities consist of radiation dose profile measurements with respect to cavities voltage, RF pulse structure and cavity position.

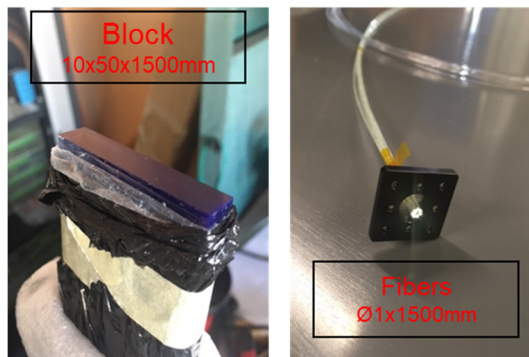


Figure 1: Plastic scintillators, block (left) and fibres bundle (right).

The current set up consist of two NaI(Tl) scintillators connected to a photo multiplier and a multichannel analyser and eight Geiger-Muller (GM) counters (LB6500-H10 connected to a LB5340 data logger). The power tests are performed mostly one cavity at the time. Six G-M are placed around the vacuum vessel close to the powered cavity, while the remaining two are always fixed at the cryomodule ends. On Figures 2 and 3 are shown their location when cavity #2 is powered, GM1 to GM6 are for low dose rate while GM7 and GM8 are for high dose rate. A neutron detector (LB6411) is installed close to the bunker wall

[†]enrico.cenni@cea.fr

(about 3 m from the beam axis). Finally a gamma ray detection system based on plastic scintillators (blocks and fibres), shown in Figure 1, has been developed allowing a pulse by pulse radiation measurement, and some of its design parameters are summarized in Table 2.

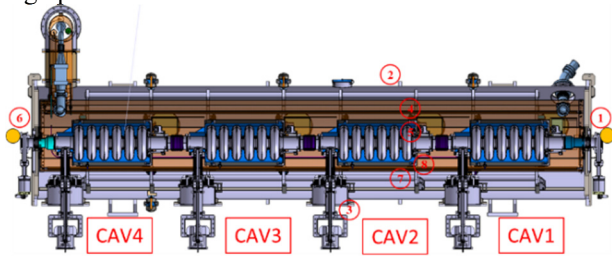


Figure 2: ESS CM, scintillators NaI(Tl) and plastic (yellow dots) and a dose rate GM detectors (numbered red circle).

Table 2: Plastic Scintillator Detection System Parameters

Parameters	Value [Block/Fibres]
Scintillator rise time [ns]	1/0.9
Scintillator decay time [ns]	3.3/2.1
Wavelength max. [nm]	435/425
Attenuation length [cm]	400/380
Refractive index	1.58
Efficiency [ph./1MeV e ⁻]	9200/10000
PM rise time [ns]	0.57
PM peak sensitivity [nm]	400
Control system rise time [μ s]	~8

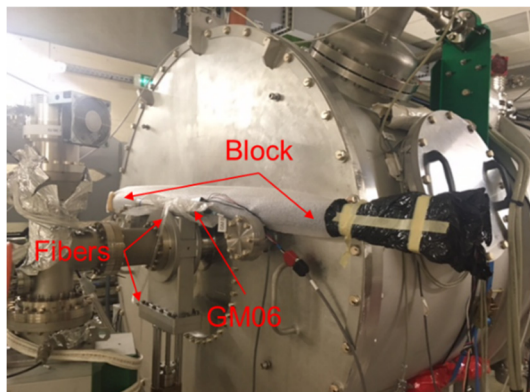


Figure 3: Plastic scintillators set up during cryomodule test, the block is on top of the beam pipe while fibres are wrapped round it, in the picture is shown the GM06 side.

DATA ANALYSIS

At first we will focus showcasing some plastic scintillators applications during CM testing and the usage of simulation tools in order to have a better understanding of field emission phenomena (*i.e.* neutron production). In Figure 4 is shown the radiation measured when the cavity is powered with a square pulse of 500 μ s reaching 20 MV/m. It shows a clear correlation between the electron current measured in the FPC and the radiation detected, meaning that part of electron produced in the FPC are able to enter the cavity and hence being accelerated. We were able to

confirm the correlation by suppressing the corresponding radiation using the FPC high voltage biasing system which inhibits electron multiplication inside de FPC.

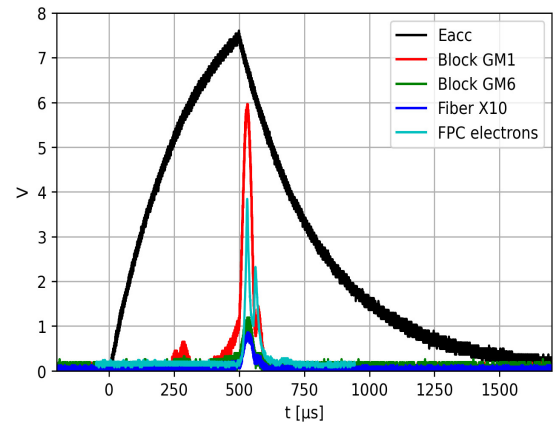


Figure 4: CM32, CAV4 excited with 500 μ s square pulse, the maximum Eacc is about 20MV/m (black). Electron current detected by the pick-up in the fundamental power coupler (cyan) and the radiation detected by the plastic scintillator at the cryomodule ends, block at GM1 position (red) block at GM6 position (green) and fiber (blue).

Figure 5 displays a second example that shows the sensitivity of the plastic scintillators system. It is clearly visible the radiation modulation due to Lorentz force detuning.

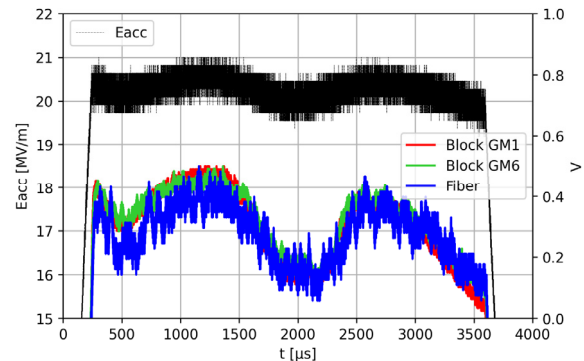


Figure 5: CM32, CAV1 excited with nominal pulse, the maximum Eacc is about 21.2 MV/m (black), radiation detected by block at GM1 position, close to cavity (red), radiation detected by block at GM6 position (green) and from fiber (blue).

Particle Tracking and Particle Shower Simulation

Part of our cryomodule testing routine consists also in data analysis by means of particle tracking code and Monte Carlo simulations. This allows us to have a better insight into field emission phenomena occurring during testing and in future operation. Typically two codes with a set of post processing tools are used, one is for electrons tracking within the cavities (based on Fishpact [7]) while the second (Geant4 [8]) allows the simulation of particle and matter interaction (*e.g.* bremsstrahlung radiation due to electron impacts).

Content from this work may be used under the terms of the CC BY 4.0 licence (© 2022). Any distribution of this work must maintain attribution to the author(s), title of the work, publisher, and DOI

The tracking code consist of a Runge-Kutta integration algorithm (4th order) of relativistic particle dynamics. Electrons trajectories are computed from the emitter (typically on the cavity iris) to the landing point. They are then used as an input for the Geant4 model. In Figure 6 is shown an example related to neutron production described in the next section. The trajectories calculated by Fishpack (Figure 8) are used in Geant4 (top of Figure 6) allowing the calculation of photon flux, radiation dose and neutron production around the cryomodule (bottom Figure 6).

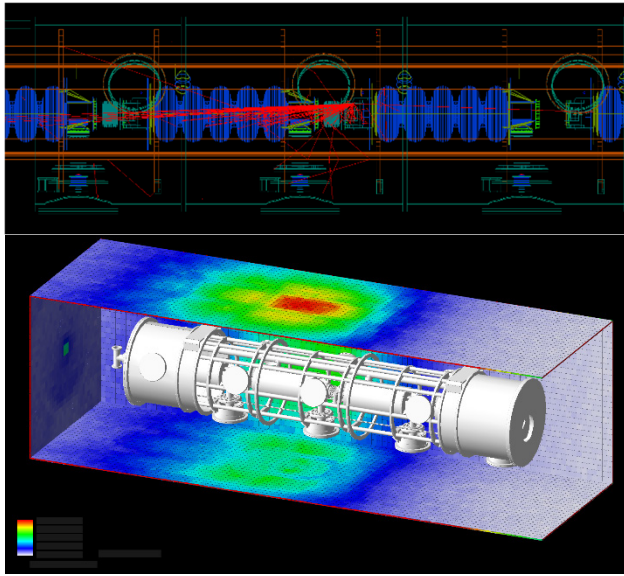


Figure 6: Cut view with electron trajectories in red (top) and photon flux (bottom) from Geant4 model.

Neutron Production

During cryomodule test we observed neutron production, in Figure 7 dose rates are reported (red bar for gamma integrated other the radial position and gray bar for neutron), cavities are powered at 20 MV/m (except for CAV1 that was limited at 17.5 MV/m) and RF pulse of 3.6 ms with 14 Hz repetition rate.

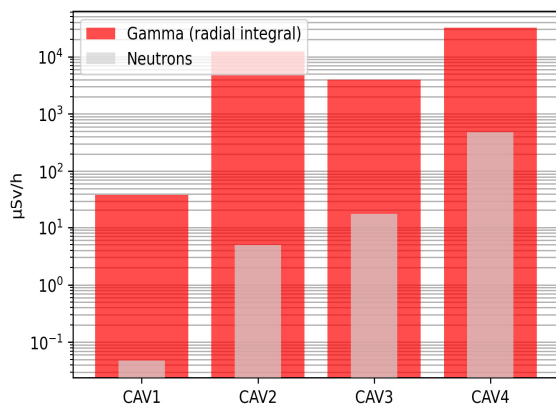


Figure 7: CM31 Dose rate over all radial detectors for photons and single point dose rate for neutrons. CAV1 is operated at 17.5MV/m, while all the other at nominal pulse.

In order to better understand the phenomenon we took advantage of the suite of codes that we normally use for field emission and high energy photons radiation.

The scenario that seems to be most probable is the following:

1. Field emission occurs in cavity position 4 (CAV4), most likely on the first iris in the second cell.
2. Electrons are accelerated by CAV4 and the impact the adjacent CAV3, as shown in Figure 8.
3. Electrons with kinetic energy between 12 and 15 MeV (when the cavity is operated at 20 MV/m) impact the cavity inner surfaces.
4. A considerable part of the electrons emitted current impact the CAV3 beam pipe towards CAV2.
5. Electrons are slowed into the Niobium of the cavity and produce bremsstrahlung radiation.
6. The produced photons have enough energy to excite the giant dipole resonance of Niobium nuclei [9,10] and produce neutrons with the following reaction $\gamma + Nb^{93} \rightarrow n + Nb^{92m}$.
7. Nb^{92m} decays with a half-life of 10.15 days emitting a photon of 934.44 keV that we observe in the gamma spectra once the cavities are powered off.

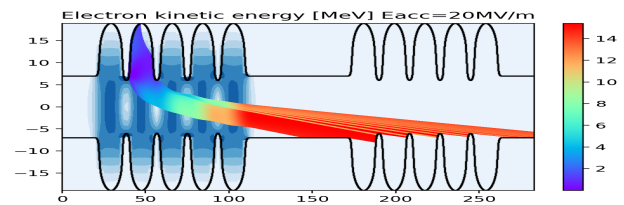


Figure 8: Electrons trajectory originated in CAV4 and impacting on CAV3, while CAV4 is operated at 20MV/m.

SUMMARY

We have implemented a set of tools in order to detect and analyse radiation produced by field-emitted electrons impacting on cavity surface. A new detections system based on plastic scintillator has been developed and deployed during cryomodule test, providing valuable information concerning the radiation generated by field emission phenomena pulse by pulse. Simulation tools have been also improved in order to model particle tracking and particle/matter interaction in a realistic cryomodule environment.

These sets of tools have proven to be valuable in order to understand field emission behaviour and its effects during cryomodule test. Some applications are showcased here: (1) Lorentz force detuning effect on the radiation pattern was observed proving the system sensitivity. (2) Possibility to observe and distinguish between the radiation generated by electrons produced in the couplers and the ones coming from cavity surface. Finally (3) neutron generation, which sometime occurs during cryomodule operation, was simulated allowing to determine the most likely activation scenario.

REFERENCES

- [1] P. Bosland *et al.*, “Tests at High RF Power of the ESS Medium Beta Cryomodule Demonstrator,” in *Proc. 10th Int. Particle Accel. Conf (IPAC'19)*, Melbourne, Australia, May 2019, pp. 1940-1943. doi:10.18429/JACoW-IPAC2019-TUPTS006
- [2] C. Maiano and E. Laface, “Field Emission Measurements at ESS Lund Test Stand,” presented at the 13th Int. Particle Accelerator Conf. (IPAC'22), Bangkok, Thailand, Jun. 2022, paper TUPOTK027, this conference.
- [3] P. Bosland, Piquet, Olivier, E. Cenni, G. Devanz, and P. Sa-huquet, “Results of the RF Power Tests of the ESS Cryomodules Tested at CEA,” presented at the 13th Int. Particle Accelerator Conf. (IPAC'22), Bangkok, Thailand, Jun. 2022, paper TUPOTK002, this conference.
- [4] E. Cenni, G. Devanz, O. Piquet, M. Baudrier, D. Roudier, and L. Maurice, “Field Emission Studies During ESS Cryomodule Tests at CEA Saclay,” in *Proc. SRF2021*, East Lansing, MI, USA, Jun.-Jul. 2021, pp. 677-681. doi:10.18429/JACoW-SRF2021-WEPTV016
- [5] E. Cenni, “Field Emission Studies on ESS Elliptical Prototype Cavities at CEA-Saclay,” in *Proc. SRF'19*, Dresden, Germany, Jun.-Jul. 2019, pp. 1147-1151. doi:10.18429/JACoW-SRF2019-THP097
- [6] G. Devanz and J. Plouin, “Conceptual Design of the Beta=0.86 Cavities for the Superconducting Linac of ESS,” in *Proc. SRF'11*, Chicago, IL, USA, Jul. 2011, paper MOPO041, pp. 180-183.
- [7] G. Wu, <https://code.google.com/archive/p/fish-pact/>
- [8] S. Agostinelli *et al.*, “Geant4—a Simulation Toolkit,” *Nucl. Instrum. Methods Phys. Res. Sect. Accel. Spectrometers Detect. Assoc. Equip.* vol. 506, p. 250, 2003.
- [9] S. S. Dietrich and B. L. Berman, “Atlas of Photoneutron Cross Sections Obtained with Monoenergetic Photons,” *At. Data Nucl. Data Tables*, vol. 38, p. 199, 1988.
- [10] A. V. Varlamov, V. V. Varlamov, D. S. Rudenko, and M. E. Stepanov, “Atlas of Giant Dipole Resonances, Parameters and Graphs of Photonuclear Reaction Cross Sections,” International Atomic Energy Agency, International Nuclear Data Committee, 1999.